Sensors and Actuators A 299 (2019) 111575

Contents lists available at ScienceDirect

Sensors and Actuators A: Physical

journal homepage: www.elsevier.com/locate/sna

A flexible piezoelectric nanogenerator using conducting polymer and silver nanowire hybrid electrodes for its application in real-time muscular monitoring system

Shubhangi Khadtare, Eui Jin Ko, Young Hoon Kim, Hyoung Seok Lee, Doo Kyung Moon *

Department of Chemical Engineering, College of Engineering, Konkuk University, 1 Hwayang-dong, Gwangjin-gu, Seoul 05029, Republic of Korea

ARTICLE INFO

Article history:
Received 20 March 2019
Received in revised form 20 August 2019
Accepted 25 August 2019
Available online 26 August 2019

Keywords:
PVDF
AgNWs
Conducting polymer
Piezoelectric nanogenerator
Muscular monitoring system

ABSTRACT

In the present work, a flexible piezoelectric nanogenerators (PNGs) using poly(vinylidene fluoride) (PVDF) as an active layer with hybrid electrode is demonstrated. Here, a poly(3,4-ethylenedioxythiophene) (PEDOT) derivative, poly(2-hexyl-2,3-dihydrothieno[3,4-b][1,4]dioxine:dodecyl sulfate (PEDOT-C_6:DS) was introduced. The polymer material has a good solubility and dispersion with organic solvents. Also, the polymer has a good electrical conductivity with hydrophobic surface and uniform conducting network on PVDF. The device performance of hybrid layer with a type of uniformly covered silver nanowire (AgNWs) network and synthesized PEDOT-C_6:DS with different concentration as an electrode has been tested. This PNG exhibit superior energy harvesting performance with maximum piezoelectric output voltage and current 7.02 V and 1.11 μA, at 8 Hz operating frequency, respectively. The fabricated hybrid electrode PNG (1.5 cm × 2.5 cm) generates a maximum output power of 1.18 μW. The fabricated PNG device is capable to lit up white LEDs and charged a commercial capacitor of 1 μF with charged voltage 2.68 V in 80 s. Further, with the results obtained it is confirmed that the 1 wt% PEDOT-C_6:DS is a promising material for hybrid electrodes in electronic applications.

1. Introduction

Energy scavenging from environment is currently a big challenge for powering small electronic devices. Energy harvesting devices converting different energy sources such as solar energy, wind energy, thermal energy, and kinetic energy into electrical energy have attracted much interest in the field of wearable electronics and self-powered monitoring devices [1–7]. Researchers have gained attention in sustainable enough self-energy power sources such as self-powered multifunctional sensors [8–10], self-powered physiological monitoring [11], self-connected nanogenerators [12], e-skin mechano-sensor [13], triboelectricity [14–16] and several energy harvesting technologies such as piezoelectric and pyroelectric, which is used for powering low power electronic devices.

Among this, piezoelectric nanogenerator (PNG) made up of organic-inorganic electrodes have placed a great demand in accessible and ecologically sustainable energy generation from ambient environment and regular human activities [17–21]. Most of the PNGs are mainly made up of inorganic materials [22–24]. These inorganic electrode PNG are complicated due to brittleness of the materials, cost intensive processing and challenging scalable large area coverage and toxic constituents. PNGs with organic piezoelectric materials have several advantages such as mechanical flexibility, lightweight, easy processing, nontoxicity, compatibility with biological tissues and cost effective [25]. It exhibits high piezoelectric output response with good durability.

Hybrid electrode plays important role in opto-electronic applications such as transparent conductive films, organic solar cells, and organic light emitting diodes [26–29]. Recently, researchers gaining attention in human motion for wearable electronic devices, especially in real time muscles monitoring system applications such as eye blinking [30], elbow [31], walking [32] muscles stretching and human index finger [33], jaws, foot stress [19] with different human body movements. The present work uses hybrid electrode consisting of AgNWs and conducting polymer poly(2-hexyl-2,3-dihydrothieno[3,4-b][1,4]dioxine:dodecyl sulfate (PEDOT-C_6:DS). AgNWs is mostly used in future display technology, touch panels, OLEDs because of its transparent nature. It is highly conductive and having low sheet resistance. Having a low sheet resistance in AgNWs have an advantage in the good reliability of the devices and

* Corresponding author.
E-mail address: dkmoon@konkuk.ac.kr (D.K. Moon).

https://doi.org/10.1016/j.sna.2019.111575
0924-4247/

in opto-electronic applications. AgNWs have excellent mechanical flexibility without a change in their conductivity due to the intrinsic flexibility of silver. AgNWs deposited on substrate have relatively low adhesion force due to effects of weak van der Waals force and limited contact area between AgNWs junctions and substrate. There are a few drawbacks with AgNWs which are, non-uniform random network structure, high surface roughness [34,35]. To overcome this issue, we used PEDOT-C_6:DS polymer which helps to covers the surface of AgNWs that will provides better conduction pathways for charge transport and collection by the electrode and reduces surface roughness. In the present work, we were used flexible PVDF as an active layer in PNG because it has piezoelectric coefficient, high thermal stability and most important β phase of PVDF possesses the largest spontaneous polarization that gives to superior piezoelectric properties which makes suitability for nanogenerator fabrication [36,37].

Herein, we have fabricated the PNG using pristine AgNWs (PPNG) and AgNWs with conducting polymer PEDOT derivatives poly(2-hexyl-2,3-dihydrothieno[3,4-b][1,4]dioxine:dodecyl sulfate (PEDOT-C_6:DS) (DPNG) as a hybrid electrode based on PVDF as an active layer. The effect of PPNG and DPNG was studied to enhance piezoelectric output. For real time monitoring system applications, it is necessary to fabricate PNGs on flexible substrate. The output characteristics of PNG was measured, while the device was actuated by a cyclic stretching-releasing agitation mechanism driven by a linear motor. Increasing the output voltage should be an effective method to improve the performance of PNG. However, the effect of actuation frequency on the piezoelectric performance was also evaluated. We were tested the PNG devices with different frequency range from 1 to 10 Hz. A maximum piezoelectric output voltage and current of DPNG were found 7.2 V and 1.11 μA, at 8 Hz respectively. At the end, the long-term stability was checked for a real application of the device. The performance of stability was maintained over 20,000 cycles suggesting DPNG is highly stable than PPNG. DPNG is also capable to charge up the capacitors 1 μF with charged voltage 2.68 V in 80 s. Output power generated from the DPNG can directly drive white light emitting diodes suggesting that it is applicable as a self-powered energy harvester.

Further, we have demonstrated the application of muscular motion monitoring by attaching the DPNG device on the finger. Recently, wearable technologies have attracted a huge attention due to the wide variety of applications ranging from health-care [38] to textile electronics [39,40]. The current wearable electronics requires external power sources such as batteries which requires periodical replacement and other drawbacks. To overcome this issue, we have made a PNG based wearable monitoring system. The DPNG device shows good flexibility to be used for the muscular monitoring system. To demonstrate the real-time use, the device was attached on the finger and the motion was monitored through the electrical response obtained through the bending and releasing of the finger. Hence, the DPNG can be a potential candidate for the use in wearable electronic application which leads to be its commercial use in the future.

2. Experiments

2.1. Materials

PVDF with thickness 80 μm purchased from Fils Co. Ltd. AgNWs (5 mg/ml in Iso- propyl alcohol) were purchased from Sigma Aldrich. PEDOT derivatives poly(2-hexyl-2,3-dihydrothieno[3,4-b][1,4]dioxine:dodecyl sulfate (PEDOT-C_6:DS) were synthesized using oxidative polymerization [41]. All the reagents are analytically pure and used without further purification.

2.2. Film preparation

Prior to deposition, PVDF substrates blow using N_2. AgNWs (5 mg/ml in isopropyl alcohol) were used as PNG device fabrication. The top electrode of the nanogenerator were prepared using spin coating. Samples were prepared using spin coater GM Spin 100. AgNWs were spin coated onto PVDF at 1000 rpm for 30 s. Then spin coated samples annealed for 60 °C for 15 min. The PEDOT-C_6:DS solution was spin coated onto AgNWs at a speed of 1000 rpm for 30 s. After PEDOT-C_6:DS deposition, the films are annealed at 60 °C for 15 min. Bottom electrode prepared using similar experimental process.

2.3. Fabrication and characterization of the PNG

PVDF film with 3×3 cm^2 in size were used for PNG. Before device measurement, films were cut to 1.5 cm × 2.5 cm. Al foil were used as contact electrode. Al foil were fixed at one side of the electrode to connect the nanogenerator with device measurements. The atomic force microscope (AFM) images were obtained on a XE-100 in a non-contact tapping mode with scan size 20×20 μm^2. Field emission scanning electron microscopy (FE-SEM) images were taken to investigate the detail surface morphological and cross-sectional characteristics of the PPNG and DPNG films using Helios Nanolab 600 and Hitachi SU8010. To know the surface wettability properties of PPNG and DPNG, contact angle measurements are carried out using KRUSS DSA 100 drop shape analyzer instrument. XRD results were obtained using a Rigaku X-ray diffractometer with CuKα radiation (wavelength 0.154 nm) operated at 40 kV and 30 mA. The samples were scanned in the 2θ range of 10–40°. Infrared spectra of the PVDF were taken FTIR spectrometer 4100 (JASCO, Japan) in the range of 700–1400 cm^{-1} with a resolution of 2 cm^{-1}, where the transmission mode was adopted in the ATR mode.

The piezoelectric output voltage was detected by directly connecting to a digital multimeter Keithley meter (Tektronix DMM 7510) with input impedance of 10 MΩ. Fixed resistances were used in a range from 1 MΩ to 11.11111 MΩ to measure the output power with a resistance decade box (RBOX-408, LUTRON). The PMC-1 HS-1 Axis motion controller series was used for the mechanical bending measurements. The motion controller was used for the movement of 0.2 mm displacement by stretching and releasing, which is 0.8% deformation ratio ($\frac{\Delta L}{L_0} \times 100$). (ΔL: displacement (0.2 mm), L0: Initial length of PNG (25 mm))

3. Results and discussion

The device structure of the fabricated PNG is shown in Fig. 1(a). The detailed fabrication steps are shown in Fig. 1(b) and process is given in experimental section. To prepare uniform film for good quality PNG, we used 1 wt% PEDOT-C_6:DS polymer dissolved in dichlorobenzene solvent. The AgNWs into PEDOT-C_6:DS polymer improves the uniformity of NWs in the polymer matrix, which enhances the stresses applied to the NWs during PNG deformation.

Fig. 1(c) shows photographs of transparency and flexibility of hybrid electrodes PNG device. Fig. 2(a–d) shows FE-SEM images of pristine AgNWs and 1 wt% AgNWs-PEDOT-C_6:DS. A randomly oriented growth of AgNWs were seen in Fig. 2(a and c). AgNWs are surrounded by small grains of 1 wt% PEDOT-C_6:DS clearly seen in Fig. 2(b and d). For 2 wt% PEDOT-C_6:DS shows that surface is fully covered with no pin holes as clearly shown in Fig. S1(a and b).

For Surface topography images of pristine AgNWs and 1 wt% AgNWs-PEDOT-C_6:DS obtained from AFM are shown in Fig. 2(g and h), respectively. These randomly oriented AgNWs have high surface roughness values 34.92 nm as shown in Fig. 2(g). There

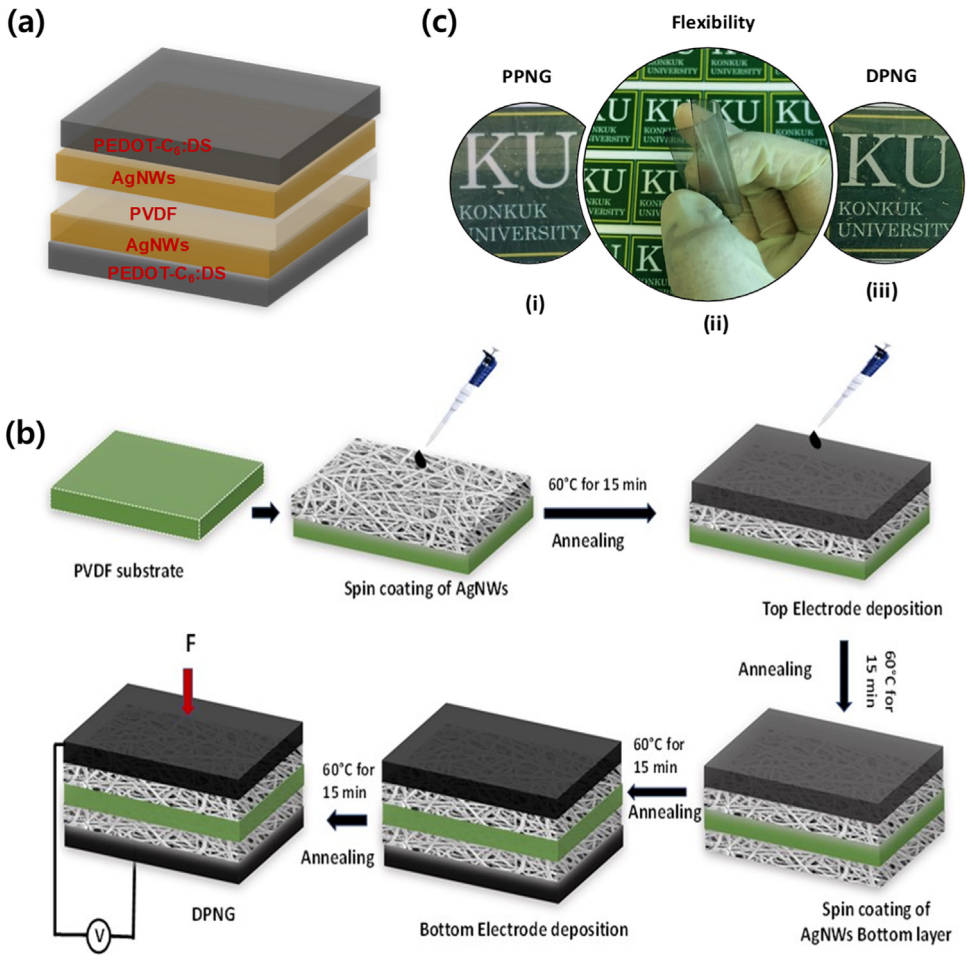

Fig. 1. (a) Schematics of DPNG (b) Schematic representation of fabrication of hybrid electrode PNG (c) Photographs of transparency of AgNWs film, Flexible PVDF based hybrid electrode PNG and transparency of hybrid electrode.

is discontinuous network of AgNWs. The surface roughness of 1 wt% PEDOT-C_6:DS was 24.70 nm. With PEDOT-C_6:DS polymer over AgNWs, surface becomes fully connected network and these AgNWs sink into the PEDOT-C_6:DS polymer which flatten out nanowires and reduces the surface roughness. As concentration of PEDOT-C_6:DS increases from 1 wt% to 2 wt%, surface roughness reduces from 24.70 to 16.60 nm, indicating that surface becoming more smoother and smoother as shown in Fig. S1(c). The thickness of entire device for wearable devices is one of the important factors due to the flexibility, application on the human body and etc [42]. Cross-sectional FE-SEM images for the thickness of the entire PPNG and 1 wt% DPNG are shown in Fig. 2(e and f). The thickness of both top and bottom electrodes of PPNG was ~100 nm with non-uniform NWs, whereas the one of 1 wt% DPNG was ~100 nm with highly covered uniform area. Therefore, the layer of AgNWs with PEDOT-C_6:DS is more appropriate than the one of AgNWs only.

Pristine AgNWs have sheet resistance 0.07 kΩ/□ whereas PEDOT-C_6:DS having sheet resistance 0.27 kΩ/□. After addition of PEDOT-C_6:DS, the sheet resistance becomes higher than pristine AgNWs, respectively. The conductivity of pristine AgNWs were 1.28×10^7 S/cm whereas PEDOT-C_6:DS having 3.59×10^7 S/cm. It is indicating that conductivity of hydride electrode DPNG is enhanced, as compared to PPNG observing improved performance in PNG. The inherent irregular surface morphology and poor adhesion makes PPNG with less PNG performance. Whereas with PEDOT-C_6:DS, the surface becomes fully covered, uniform with good adhesion and pinhole free, so observed better PNG device performance.

As shown in Fig. S2(a), the black-line XRD pattern of PVDF film annealed at 90° indicates peaks at 17.8°, 18.4°, 19.9° and 26.5°, which confirms the α-phase of PVDF. The pattern of red-line indicates peaks at 20.6° and 36.6° corresponding to the β-phase of PVDF substrate that used in this study. In order to confirm the β-phase of PVDF substrate clearly, ATR-FTIR was taken as well. As shown in Fig. S2(b), the peaks for α-phase were detected at 765, 796, and 976 cm^{-1} and the peaks for β-phase were indicated at 840 and 1280 cm^{-1}. PVDF substrate introduced in this study showed high β-phase, which is good for high piezoelectric performance [43,44].

A water contact angle measurement was carried out to check the substrate wettability and roughness with water droplet. The hydrophobic ability of the film is an important factor for the performance of the PNGs [45]. The measured water contact angle of pristine AgNWs film is 81.3°, as shown in Fig. S3(a) indicating that pristine AgNWs indicates rough surface of the film comprised of nanowires and hydrophilic in nature [46]. Increase of contact angle is observed with AgNWs- PEDOT-C_6:DS is 92.5° because the AgNWs is embedded into PEDOT-C_6:DS polymer matrix (as shown in Fig. S3(b)) and showing hydrophobic in nature. We concluded that as contact angles increases with decrease in surface roughness as we clearly seen in AFM results [47]. Contact angle and surface energy values of AgNWs and AgNWs- PEDOT-C_6:DS are tabulated in Table S1.

The frequency response of 1 Hz to 10 Hz of output voltage obtained with PNG are measured and depicted in Fig. 3, respectively. Frequency dependent performance of piezoelectric micro generator and high acceleration based on PZT materials previously

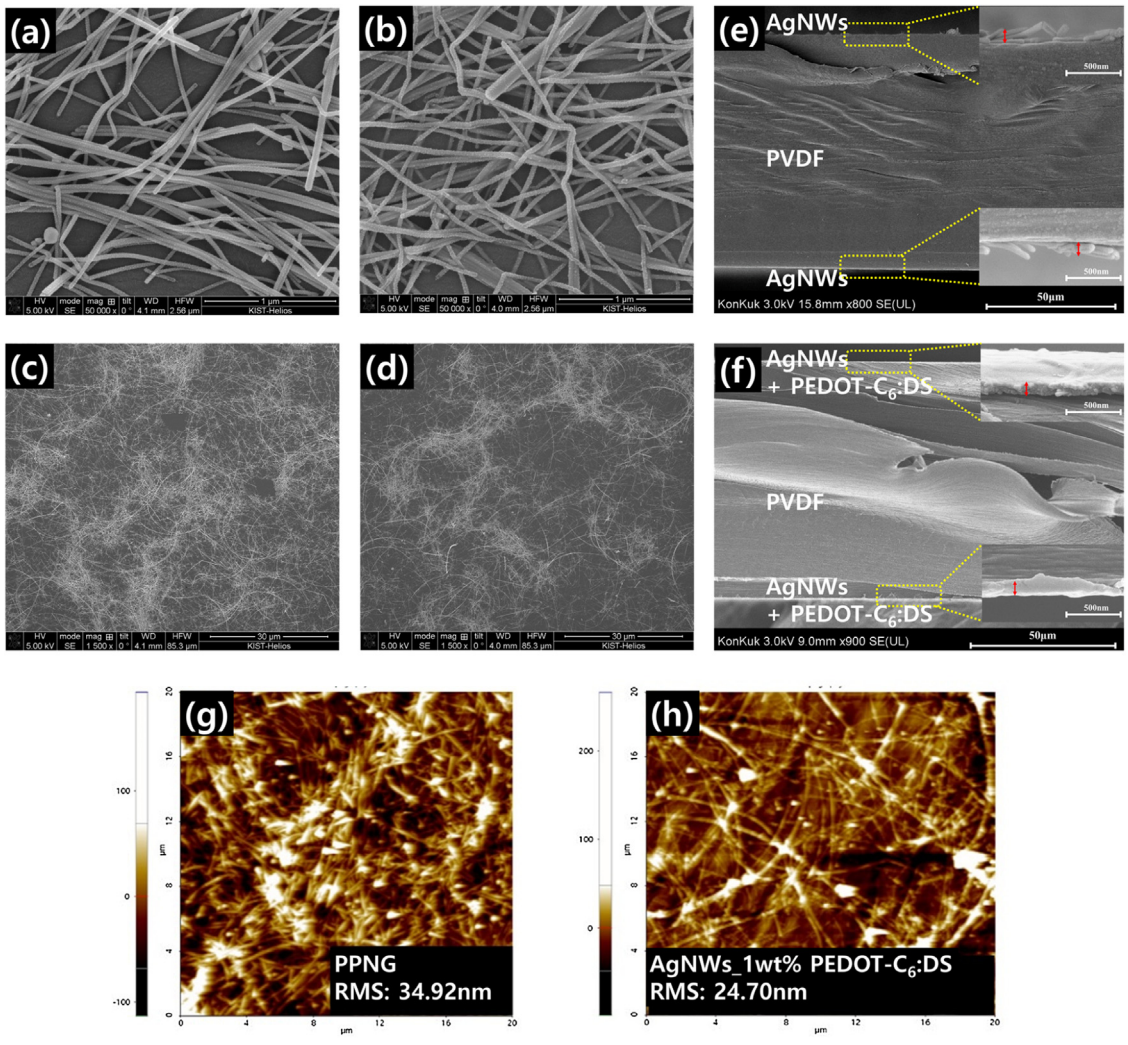

Fig. 2. FE-SEM images of (a, c) PPNG and (b, d) 1 wt% DPNG, cross-section images of (e) PPNG and (f) 1 wt% DPNG (inset: enlarged images). AFM images of (g) PPNG and (h) 1 wt% DPNG.

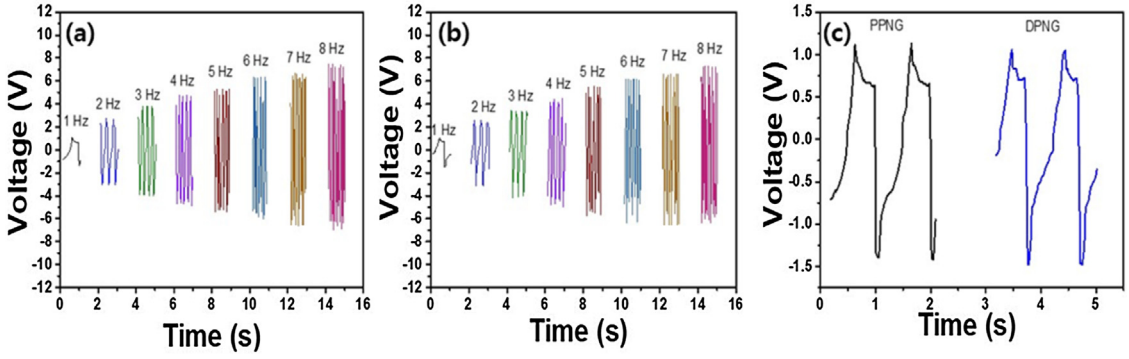

Fig. 3. Frequency dependent output voltage of (a) PPNG (b) 1 wt% DPNG and (c) First two initial signal of output voltage of PPNG and DPNG at 1 Hz frequency.

reported by Tang et al. [48] Radeef et al. also demonstrated the great performance in harvesting the energy at low acceleration and in a low frequency environment of non-ferroelectric nanogenerator $0.7PbZn_{0.3}Ti_{0.7}O_3$-$0.3Na_2TiO_3$. Piezoelectric output voltage at different frequencies ranging from 1 to 7 Hz of PPNG, 1 wt% DPNG and 2 wt% DPNG as shown in Fig. S4. Output voltage as a function of time at higher frequencies 9 Hz and 10 Hz of PPNG are 7.36 V and 7.58 V, whereas 1 wt% DPNG are 7.50 V and 7.83 V are shown in Fig. S5(a and b). Hoque et al. also studied frequency dependent output voltage of biowaste crab shell-extracted chitin nanofiber PNGs [49,50]. The output voltage gradually increased with the increase in the frequency of PPNG and 1 wt% DPNG device as shown in Fig. 3(a and b). Initial first two signals of the piezoelectric output voltage of PPNG and DPNG were shown in Fig. 3(c). PPNG shows that as frequency increases from 1 Hz to 8 Hz, output voltage increases from 1.41 to 6.58 V as shown in Table S2.

For 8 Hz PPNG, shows good negative output voltage 6.58 V. With further increase in frequency after 8 Hz, the output voltage signal

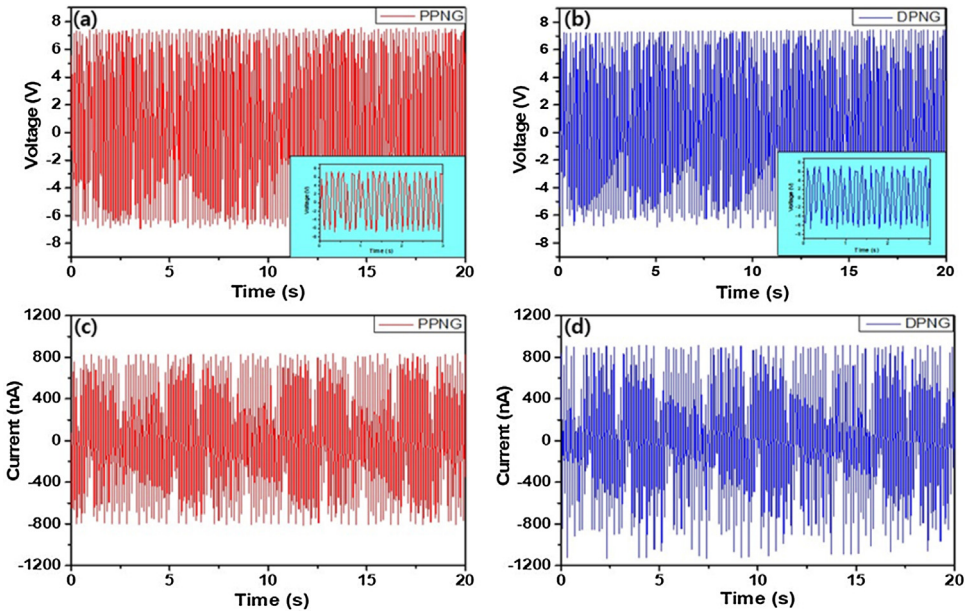

Fig. 4. Highest generated piezoelectric output voltage of (a) PPNG (inset shows magnified view of PPNG in 0–3 s) (b) Output voltage of DPNG (inset shows magnified view of DPNG in 0–3 s) (c) Output current of PPNG and (d) Output current of DPNG at 8 Hz frequency.

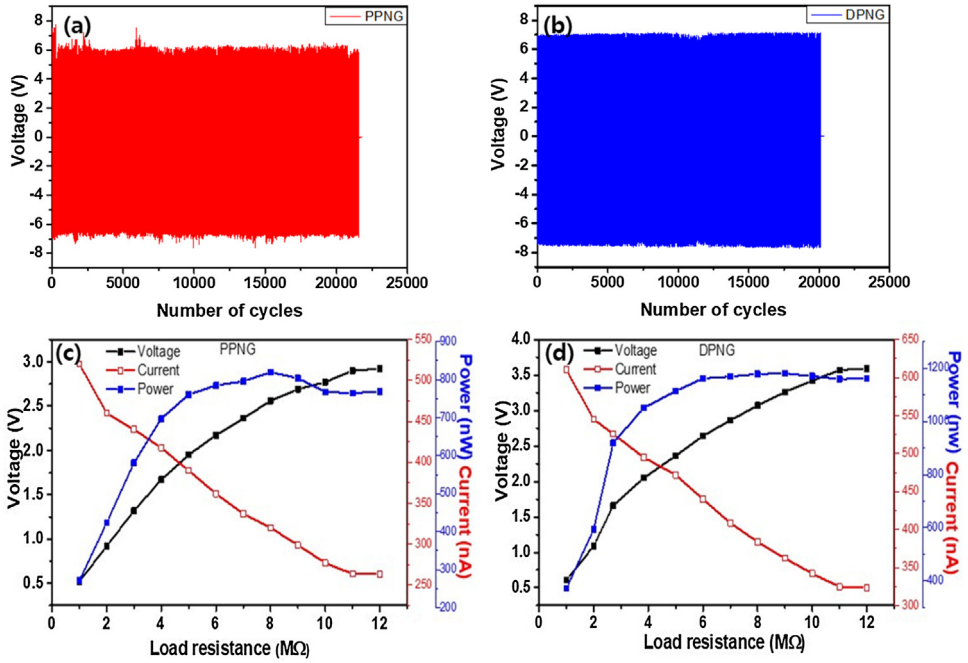

Fig. 5. (a) Long term voltage stability of PPNG over 20,000 cycles at 8 Hz actuation frequency (b) Long term voltage stability of 1 wt% DPNG over 20,000 cycles at 8 Hz actuation frequency (c) Output voltage as a function of load resistance at 8 Hz operating frequency of PPNG and (d) Output voltage as a function of load resistance at 8 Hz operating frequency of 1 wt% DPNG.

of PPNG not uniform and behavior of peak pattern is not constant. It means that the device gets depolarized after 8 Hz operating frequency. Since, polarization is an important factor that is influential to the performance of PVDF based PNG. With 1 wt% DPNG, we observed a maximum output voltage 7.02 V at 8 Hz operating frequency. 1 wt% DPNG shows higher output voltage in the case of 9 and 10 Hz, but the peak pattern is completely discrete. This result confirms that the PPNG and 1 wt% DPNG device works actively at a maximum frequency of 8 Hz. The further analysis such as maximum power calculation, commercial capacitor charging, and LED lit up were performed at 8 Hz frequency. The frequency dependent response of 2 wt% DPNG, long term stability and load resistance as a function of output voltage as shown in Fig. S6(a–c). In case of 2 wt% DPNG, the output voltage increases from 1 Hz to 5 Hz. It will go increasing as we increase frequency from 1 Hz to 5 Hz. After 5 Hz, it suddenly drops to 5.02 V showing peak pattern behavior is not consistent as we increase the frequency upto 8 Hz. Therefore, 1 wt% DPNG shows better PNG performance as compared to 2 wt% DPNG.

The highest output characteristics of as fabricated PNG was shown in Fig. 4. The average output values of voltage and current were 6.58 V and 0.81 μA at 8 Hz for the PPNG as shown

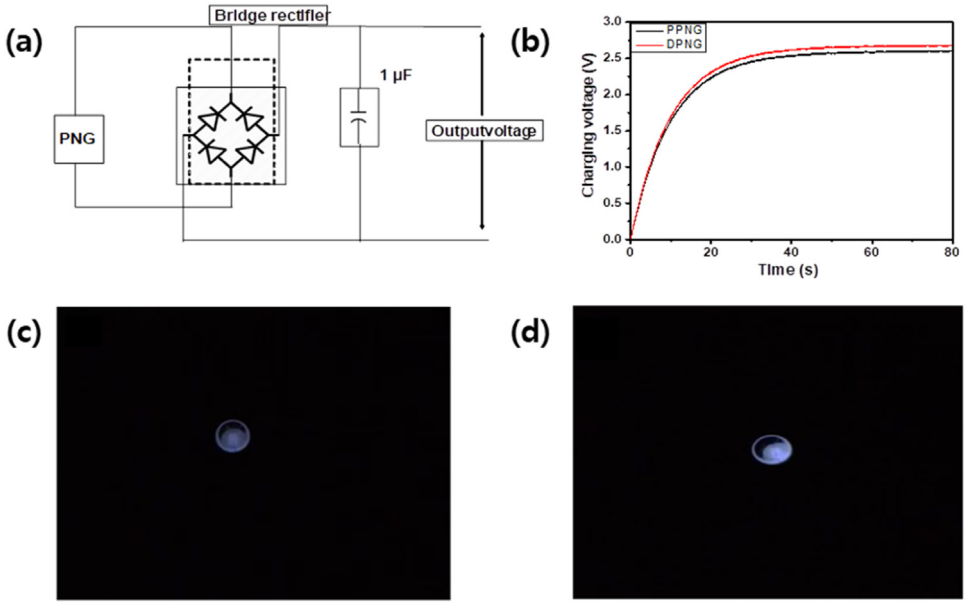

Fig. 6. (a) Schematic rectifying diagram of capacitor charging (b) Charging behavior of capacitors through PPNG and DPNG (c) Photographs of LEDs glowing using PPNG (d) Photographs of LEDs glowing using DPNG.

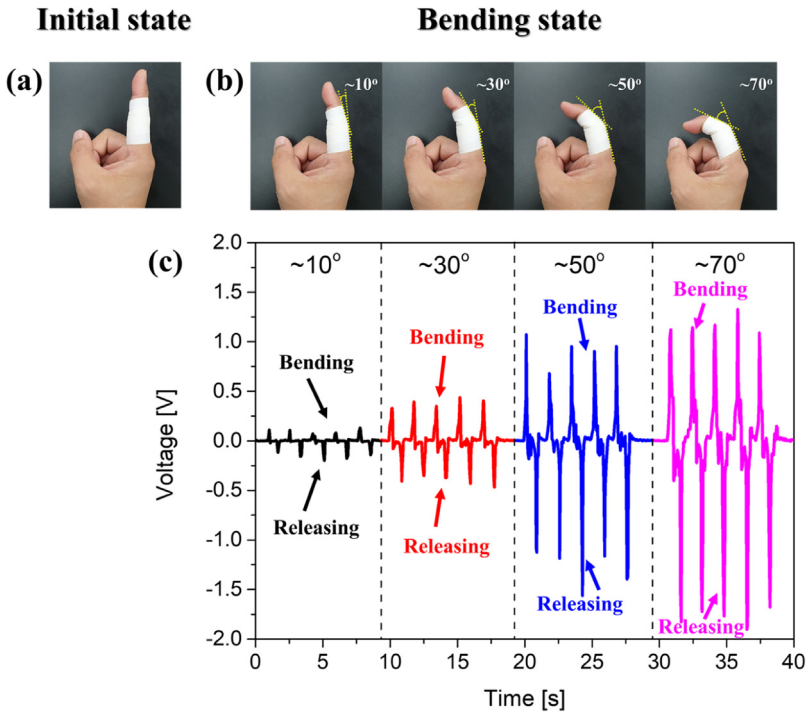

Fig. 7. (a) Photographs of human index finger using PNG (a, b) Performance of flexible DPNG under index finger movement (c).

in Fig. 4(a and c). However, with 1 wt % DPNG were 7.02 V and 1.11 μA as shown in Fig. 4(b and d). We observed improved piezoelectric output response with 1 wt% DPNG than PPNG because of low surface roughness and hydrophobic nature of PEDOT-C_6:DS polymer. The magnified view of output voltage of PPNG and DPNG in the 0–3 s, as shown in Fig. 4(a and b) inset. Piezoelectric output voltage of PPNG at 8 Hz, 9 Hz and 10 Hz are shown in Fig. S7.

To check the durability of the PNG device, a long-term stability test was carried out with PPNG and 1 wt% DPNG over the period of 20,000 cycles [51–53]. The device stability of PPNG is not good due to discontinuous network of AgNWs as shown in Fig. 5(a). The results indicated that stability of the DPNG devices was good as shown in Fig. 5(b). It means compatibility of DPNG devices is good over 20,000 cycles under an actuation frequency of 8 Hz. The devices were found rigorous and highly stable with DPNG than PPNG. DPNG with 2 wt% concentration showing stability over 400 cycles at 8 Hz as shown in Fig. S6(b). 1 wt% DPNG shows stability over 20,000 cycles which is 50 times higher than 2 wt% DPNG.

To know the effective electric power of PNG, we measured resistance using different values of the external load resistance from 1 MΩ to 11.11111 MΩ. The output voltage increased with the load resistance of PPNG as shown in Fig. 5c. The maximum instantaneous power of PPNG was about 0.81 μW, whereas the maximum instantaneous power of 1 wt% DPNG was about 1.18 μW as shown in Fig. 5(d). Obviously, the voltage increased with increasing the load resistance whereas the current decreased due to the ohmic loss. The piezoelectric characteristics output voltage, output current, maximum power and impedance matching of PPNG, 1 wt% DPNG and 2 wt% DPNG are shown in Table S3. The maximum output obtained by 1 wt% DPNG device is at 9 MΩ load resistance. These results are in good agreement with low-frequency vibration ZnO nanorods based tuning fork piezoelectric nanogenerator [54]. To demonstrate the real-time working ability of the PPNG and 1 wt% DPNG device, commercial capacitor of 1μF was charged and a white LED was lit up. Fig. 6(a) shows the circuit diagram of capacitor charging used for the demonstration. The capacitor was charged with a voltage of 2.60 V (PPNG) and 2.68 V (DPNG) at 8 Hz respectively over a period of 80 s which is shown in Fig. 6(b). Also, white LEDs were blink up using the PPNG and DPNG device (see Movie S1). The LED lit up was shown in Fig. 6(c and d), where the LED driven using PPNG lit up at low intensity. This is due to its less electrical output compared to DPNG which has more output. This makes the LED to lit up brighter with DPNG device as compared to PPNG.

The real-time application of 1 wt% DPNG as a muscular monitoring system is shown in Fig. 7. To demonstrate this application, the device is attached on the finger as shown in Fig. 7(a). When the finger gets bending and releasing, the electrical signal in the positive and negative sides appears to the corresponding movement. When the finger bends, a force acts on the device leads to the changes in alignment of dipoles in the PVDF active layer. This leads to the development of piezoelectric potential and the electrons moves from one side of electrode to other side of the electrode. This could be analyzed by appearing a peak at positive side. When the finger gets released, the electron flow gets reversed due the force release and the dipole reversal. The negative peak appears at this time. As shown in Fig. 7(c), when the bending angle is increased from $\tilde{1}0^{\circ}$ to $\tilde{7}0^{\circ}$, the average output voltage is gradually increased, 0.18 V ($\tilde{1}0^{\circ}$), 0.43 V ($\tilde{3}0^{\circ}$), 1.2 V ($\tilde{5}0^{\circ}$), and 1.82 V ($\tilde{7}0^{\circ}$), respectively. With the change of bending angle of index finger, it showed high sensitivity. This results are similar to the application of cowpea-structured PVDF/ZnO nanofibers based self-powered piezoelectric bending motion sensor under various bending angles by Deng et al. [55]. The supporting video is shown in Movie S2. The results proved that DPNG device can be used as a muscular monitoring system to monitor or diagnose the muscles in various parts of the human body. Moreover, the devices are adaptable to various other locations in the human body and sensitive to the human body motions.

4. Conclusions

In summary, we demonstrated the high performance PNG based on flexible PVDF as an active layer. We successfully fabricated device using pristine AgNWs and the PEDOT-C_6:DS polymer as a hybrid electrode. The optimized device frequency is 8 Hz. After 8 Hz, we observed the piezoelectric output voltage peak pattern is not uniform. Further, we have performed frequency dependent electrical analysis of the 1 wt% DPNG device and noticed an outstanding output voltage of 7.02 V and a current of 1.11 μA. whereas, with the PPNG generates a maximum voltage of 6.58 V and current of 0.81 μA. The instantaneous power density is 0.81 μW for PPNG and 1.18 μW for DPNG. The as fabricated DPNGs exhibit outstanding long-term mechanical stability with excellent performances over 20,000 cycles. The FE-SEM images shows AgNWs fully covered by PEDOT-C_6:DS polymer and surface becomes smoother, so we observed better output piezoelectric response of DPNG. The generated electric power of 1 wt% DPNG was capable to charge a commercial capacitor of 1 μF with voltage of 2.68 V for 80 s at 8 Hz and able to light up a white LED. PNGs with index finger are fabricated to form a self-powered muscles monitoring system. This muscular monitoring system can transform the mechanical energy of the fingers into electrical signal with the advantages of environmentally and ecofriendly, simple fabrication steps with piezoelectric response. Further with its usage in the real-time muscular monitoring system the device proved its capability in the potential application and its possibility to use commercially in the health-care field for treatment and diagnosis. This type of batteryless technology will be a breakthrough in near future in the field of wearable electronic technology.

Acknowledgements

This research was supported by the New & Renewable Energy Core Technology Program of the Korea Institute of Energy Technology Evaluation and Planning (KETEP) grant funded by the Ministry of Trade, Industry and Energy, Republic of Korea (No. 20153010140030) and the Human Resources Program in Energy Technology of the Korea Institute of Energy Technology Evaluation and Planning (KETEP), granted financial resource from the Ministry of Trade, Industry and Energy, Republic of Korea (No. 20194010201790). This paper was supported by Konkuk University Researcher Fund in 2018.

Appendix A. Supplementary data

Supplementary material related to this article can be found, in the online version, at doi:https://doi.org/10.1016/j.sna.2019.111575.

References

[1] Y.F. Hua, Z.L. Wang, Recent progress in piezoelectric nanogenerators as a sustainable power source in self-powered systems and active sensors, Nanoenergy 14 (2015) 3–14.
[2] Y. Zi, Z.L. Wang, Nanogenerators: an emerging technology towards nanoenergy, APL Mater. 5 (2017) 074103–074113.
[3] J. Briscoe, S. Dunn, Piezoelectric nanogenerators – a review of nanostructured piezoelectric energy harvesters, Nanoenergy 14 (2015) 15–29.
[4] S. Stassi, V. Cauda, C. Ottone, A. Chiodoni, C.F. Pirri, G. Canavese, Flexible piezoelectric energy nanogenerator based on ZnO nanotubes hosted in a poly carbonate membrane, Nanoenergy 13 (2015) 474–481.
[5] Z. Wen, M.H. Yeh, H. Guo, J. Wang, Y. Zi, W. Xu, J. Deng, L. Zhu, X. Wang, C. Hu, L. Zhu, X. Sun, Z.L. Wang, Self-powered textile for wearable electronics by hybridizing fiber-shaped nanogenerators, solar cells and supercapacitors, Sci. Adv. 2 (2016) e1600097, 1-8.
[6] S. Lee, S.H. Bae, L. Lin, Y. Yang, C. Park, S.W. Kim, S.N. Cha, H. Kim, Y.J. Park, Z.L. Wang, Super-flexible nanogenerator for energy harvesting from gentle wind and as an active deformation sensor, Adv. Funct. Mater. 23 (2012) 2445–2449.
[7] W. Seung, M.K. Gupta, K.Y. Lee, K.S. Shin, J.H. Lee, T.Y. Kim, S. Kim, J. Lin, J.H. Kim, S.W. Kim, Nanopatterned textile-based wearable triboelectric nanogenerator, ACS Nano 9 (2015) 3501–3509.
[8] K. Maity, D. Mandal, All-organic high-performance piezoelectric nanogenerator with multilayer assembled electrospun nanofiber Mats for self-powered multifunctional sensors, ACS Appl. Mater. Interfaces 10 (2018) 18257–18269.
[9] X. Chen, X. Li, J. Shao, N. An, H. Tian, C. Wang, T. Han, L. Wang, B. Lu, High-performance piezoelectric nanogenerators with imprinted P(VDF-TrFE)/$BaTiO_3$ nanocomposite micropillars for self-powered flexible sensors, Small 13 (2017) 1604245, 1-12.
[10] X. Chen, J. Shao, N. An, X. Li, H. Tian, C. Xu, Y. Ding, Self-powered flexible pressure sensors with vertically well-aligned piezoelectric nanowire arrays for monitoring vital signs, J. Mater. Chem. C 3 (2015) 11806–11814.
[11] X. Chen, K. Parida, J. Wang, J. Xiong, M.-F. Lin, J. Shao, P.S. Lee, A Stretchable and transparent nanocomposite nanogenerator for self-powered physiological monitoring, ACS Appl. Mater. Interfaces 9 (2017) 42200–42209.
[12] X. Chen, H. Tian, X. Li, J. Shao, Y. Ding, N. An, Y. Zhou, A high performance P(VDF-TrFE) nanogenerator with self-connected and vertically integrated fibers by patterned EHD pulling, Nanoscale 7 (2015) 11536–11544.

[13] B. Dutta, E. Kar, N. Bose, S. Mukherjee, NiO@SiO_2/PVDF: a flexible polymer nanocomposite for a high performance human body motion-based energy harvester and tactile e-skin mechanosensor, ACS Sustain. Chem. Eng. 6 (8) (2018) 10505–10516.
[14] J. Song, B. Yang, W. Zeng, Z. Peng, S. Lin, J. Li, X. Tao, Highly flexible, large-area, and facile textile-based hybrid nanogenerator with cascaded piezoelectric and triboelectric units for mechanical energy harvesting, Int. J. Adv. Mater. Technol. 3 (1800016) (2018) 1–15.
[15] B. Dudem, D.H. Kim, A.R. Mule, J.S. Yu, Enhanced performance of microarchitectured PTFE-Based triboelectric nanogenerator via simple thermal imprinting lithography for self-powered electronics, ACS Appl. Mater. Interfaces 10 (2018) 24181–24192.
[16] Z.L. Wang, Triboelectric nanogenerators as new energy technology for self-powered systems and as active mechanical and chemical sensors, ACS Nano 7 (11) (2013) 9533–9557.
[17] V. Vivekananthan, N.R. Alluri, Y. Purusothaman, A. Chandrasekhar, S.J. Kim, A flexible, planar energy harvesting device for scavenging road side waste mechanical energy via the synergistic piezoelectric response of $K_{0.5}Na_{0.5}NbO_3$-$BaTiO_3$/PVDF composite films, Nanoscale 9 (2017) 15122–15130.
[18] L. Jin, J. Tao, R. Bao, L. Sun, C. Pan, Self-powered real-time movement monitoring sensor using triboelectric nanogenerator technology, Sci. Rep. 7 (2017) 1–6.
[19] N.R. Alluri, V. Vivekananthan, A. Chandrasekhar, S.J. Kim, Adaptable piezoelectric hemispherical composite strips using a scalable groove technique for a self-powered muscle monitoring system, Nanoscale 10 (2018) 907–913.
[20] S. Xu, Y. Qin, C. Xu, Y. Wei, R. Yang, Z.L. Wang, Self-powered nanowire devices, Nat. Nanotechnol. 5 (2010) 366–372.
[21] C. Opoku, A.S. Dahiya, C. Oshman, F. Cayrel, G. Poulin-Vittrant, D. Alquier, N. Camara, Fabrication of ZnO nanowire based piezoelectric generators and related structures, Phys. Procedia 70 (2015) 858–862.
[22] A. Sultana, M.M. Alam, S. Garain, T.K. Sinha, T.R. Middy, D. Mandal, Organo-lead halide perovskite induced electroactive β-phase in porous PVDF films: an excellent material for photoactive piezoelectric energy harvester and photodetector, ACS Appl. Mater. Interfaces 7 (2015) 4112–4130.
[23] M.M. Alam, A. Sultana, D. Mandal, Biomechanical and acoustic energy harvesting from TiO_2 nanoparticle modulated PVDF nanofiber made high performance nanogenerator, ACS Appl. Energy Mater. 1 (2018) 3103–3112.
[24] S.M. Jeong, J.H. Kim, S. Song, J. Seo, J.I. Hong, N.Y. Ha, H. Takezoe, D.J. Jeong, H. Kim, Conductive, flexible transparent electrodes based on mechanically rubbed nonconductive polymer containing silver nanowires, RSC Adv. 5 (2015) 51086–51091.
[25] D. Chen, F. Zhao, K. Tong, G. Saldanha, C. Liu, Q. Pei, Mitigation of electrical failure of silver nanowires under current flow and the application for long lifetime organic light-emitting diodes, Adv. Electron. Mater. 2 (2016) 1600167–1600177.
[26] N. Ye, J. Yan, S. Xie, Y. Kong, T. Liang, H. Chen, M. Xu, Silver nanowire–graphene hybrid transparent conductive electrodes for highly efficient inverted organic solar cells, Nanotechnology 28 (2017) 305402–305410.
[27] S. Kim, S.Y. Kim, J. Kim, J.H. Kim, Highly reliable AgNW/PEDOT: PSS hybrid films: efficient methods for enhancing transparency and lowering resistance and haziness, J. Mater. Chem. C 2 (2014) 5636–5643.
[28] S.H. Lee, S. Lim, H. Kim, Smooth-surface silver nanowire electrode with high conductivity and transparency on functional layer coated flexible film, Thin Solid Films 589 (2015) 403–407.
[29] L. Lian, X. Xi, D. Dong, G. He, Highly conductive silver nanowire transparent electrode by selective welding for organic light emitting diode, Org. Electron. 60 (2018) 9–15.
[30] S. Lee, S.H. Bae, L. Lin, Y. Yang, C. Park, S.W. Kim, S.N. Cha, H. Kim, Y.J. Park, Z.L. Wang, Super-flexible nanogenerator for energy harvesting from gentle wind and as an active deformation sensor, Adv. Funct. Mater. 23 (2013) 2445–2449.
[31] C. Zhang, Y. Fan, H. Li, Y. Li, L. Zhang, S. Cao, S. Kuang, Y. Zhao, A. Chen, G. Zhu, Z.L. Wang, Fully rollable lead-free poly(vinylidene fluoride)-niobate-based nanogenerator with ultra-flexible nano-network electrodes, ACS Nano 12 (2018) 4803–4811.
[32] J. Wang, S. Li, F. Yi, Y. Zi, J. Lin, X. Wang, Y. Xu, Z.L. Wang, Sustainably powering wearable electronics solely by biomechanical energy, Nat. Commun. 7 (1–8) (2016) 12744.
[33] R. Yang, Y. Qin, C. Li, G. Zhu, Z.L. Wang, Converting biomechanical energy into electricity by a muscle-movement-driven nanogenerator, Nano Lett. 9 (2009) 1201–1205.
[34] J. Gu, X. Wang, H. Chen, S. Yang, H. Feng, X. Ma, H. Ji, J. Wei, M. Li, Conductivity enhancement of silver nanowire networks via simple electrolyte solution treatment and solvent washing, Nanotechnology 29 (1-10) (2018) 265703.
[35] S. Lee, S. Shin, S. Lee, J. Seo, J. Lee, S. Son, H.J. Cho, H. Algadi, S. Al-Sayari, D.E. Kim, T. Lee, Ag nanowire reinforced highly stretchable conductive fibers for wearable electronics, Adv. Funct. Mater. 25 (2015) 3114–3121.
[36] A.J. Lovinger, Ferroelectric polymers, Science 220 (1983) 1115–1121.
[37] B.S. Ince-Gunduz, R. Alpern, D. Amare, J. Crawford, B. Dolan, S. Jones, R. Kobylarz, M. Reveley, P. Cebe, Impact of nanosilicates on poly(vinylidene fluoride) crystal polymorphism: Part 1. Melt-crystallization at high supercooling, Polymer 51 (2010) 1485–1493.
[38] M. Kim, Y.S. Wu, E.C. Kan, J. Fan, Breathable and flexible piezoelectric ZnO @ PVDF fibrous nanogenerator for wearable applications, Polymer 10 (1–15) (2018) 745.
[39] E. Nilsson, L. Mateu, P. Spies, B. Hagström, Energy harvesting from piezoelectric textile fibers, Procedia Eng. 87 (2014) 1569–1572.
[40] A. Lund, K. Rundqvist, E. Nilsson, L. Yu, B. Hagström, C. Müller, Energy harvesting textiles for a rainy day: woven piezoelectrics based on melt-spun PVDF microfibres with a conducting core, Npj Flex. Electron. 9 (2018) 1–9.
[41] E.J. Ko, S.J. Jeon, Y.W. Han, S.Y. Jeong, C.Y. Kang, T.H. Sung, K.W. Seong, D.K. Moon, Synthesis and characterization of nanofiber-type hydrophobic organic materials as electrodes for improved performance of PVDF-based piezoelectric nanogenerators, Nanoenergy 58 (2019) 11–22.
[42] C. Yan, W. Deng, L. Jin, T. Yang, Z. Wang, X. Chu, H. Su, J. Chen, W. Yang, Epidermis-inspired ultrathin 3D cellular sensor array for self-powered biomedical monitoring, ACS Appl. Mater. Interfaces 10 (2018) 41070–41075.
[43] L. Jin, S. Ma, W. Deng, C. Yan, T. Yang, X. Chu, G. Tian, D. Xiong, J. Lu, W. Yang, Polarization-free high-crystallization β-PVDF piezoelectric nanogenerator toward self-powered 3D acceleration sensor, Nano Energy 50 (2018) 632–638.
[44] Guo Tian, Weili Deng, Yuyu Gao, Cheng Yan Da Xiong, Xuebing He, Tao Yang, Long Jin, Xiang Chu, Haitao Zhang, Wei Yan, Weiqing Yang, Rich lamellar crystal baklava-structured PZT/PVDF piezoelectric sensor toward individual table tennis training, Nano Energy 59 (2019) 574–581.
[45] J. Li, C. Zhao, K. Xia, X. Liu, D. Li, J. Han, Enhanced piezoelectric output of the PVDF-TrFE/ZnO flexible piezoelectric nanogenerator by surface modification, Appl. Surf. Sci. 463 (2019) 626–634.
[46] Y. Xu, X. Wei, C. Wang, J. Cao, Y. Chen, Z. Ma, Y. You, J. Wan, X. Fang, X. Chen, Silver nanowires modified with PEDOT: PSS and graphene for organic light-emitting diodes anode, Sci. Rep. 7 (45392) (2017) 1–7.
[47] N. Ismail, R. Ismail, N.K.A.N. Ubaidillah, A. Jalar, N.M. Zain, Surface roughness and wettability of SAC/CNT lead free solder, Mater. Sci. Forum 857 (2016) 73–75.
[48] G. Tang, B. Yang, C. Hou, G. Li, J. Liu, X. Chen, C. Yang, A piezoelectric micro generator worked at low frequency and high acceleration based on PZT and phosphor bronze bonding, Sci. Rep. 6 (2016) 1–10.
[49] Z. Radeef, C.W. Tong, O.Z. Chao, K.S. Yee, Energy harvesting based on a novel piezoelectric 0.7$PbZn_{0.3}Ti_{0.7}O_3$-0.3Na_2TiO_3 nanogenerator, Energies 10 (646) (2017) 1–15.
[50] N.A. Hoque, P. Thakur, P. Biswas, M.M. Saikh, S. Roy, B. Bagchi, S. Das, P.P. Ray, Biowaste crab shell-extracted chitin nanofiber based superior piezoelectric nanogenerator, J. Mater. Chem. A 6 (2018) 13848–13858.
[51] M.A. Johar, M.A. Hassan, A. Waseem, J.S. Ha, J.K. Lee, S.W. Ryu, Stable and high piezoelectric output of GaN nanowire-based lead-free piezoelectric nanogenerator by suppression of internal screening, Nanomaterials 8 (6) (2018) 437, 1-12.
[52] S.Y. Chung, S. Kim, J.H. Lee, K. Kim, S.W. Kim, C.Y. Kang, S.J. Yoon, Y.S. Kim, All-solution-processed flexible thin film piezoelectric nanogenerator, Adv. Mater. 24 (2012) 6022–6027.
[53] S. Siddiqui, D.I. Kim, E. Roh, L.T. Duy, T.Q. Trung, M.T. Nguyen, N.E. Lee, A durable and stable piezoelectric nanogenerator with nanocomposite nanofibers embedded in an elastomer under high loading for a self-powered sensor system, Nanoenergy 30 (2016) 434–442.
[54] W. Deng, L. Jin, Y. Chen, W. Chu, B. Zhang, H. Sun, D. Xiong, Z. Lv, M. Zhu, W. Yang, An enhanced low-frequency vibration ZnO nanorod-based tuning fork piezoelectric nanogenerator, Nanoscale 10 (2018) 843–847.
[55] W. Deng, T. Yang, L. Jin, C. Yan, H. Huang, X. Chu, Z. Wang, D. Xiong, G. Tian, Y. Gao, H. Zhang, W. Yang, Cowpea-structured PVDF/ZnO nanofibers based flexible self-powered piezoelectric bending motion sensor towards remote control of gestures, Nano Energy 55 (2019) 516–525.

Biographies

Shubhangi Khadtare received her M. Sc (2008) and Ph.D. (2015) degrees in Physics from the Savitribai Phule Pune University, India. After completing her Ph.D., She worked as a SERB Overseas Postdoctoral Fellow at Hanyang University, South Korea (2017–2018). She currently post-doctoral fellow at Department of Materials Chemistry and Engineering, Konkuk University, South Korea. Her research areas include deposition of metal oxide thin films, fabrication and integration of piezoelectric nanodevices and systems, self-powered muscles monitoring systems, self-powered wearable systems, water splitting and energy technology solar cells.

Eui Jin Ko received his B.S. degree from the Department of Materials Chemistry and Engineering, Konkuk University, Korea in 2012. He is currently a Ph.D. candidate in the Nano & Information Materials Laboratory, Department of Chemical Engineering, Konkuk University, Republic of Korea under Prof. Doo Kyung Moon's supervision. His research interests are in conducting polymers and piezoelectric nanogenerators.

Young Hoon Kim received his B.S. degree from the Department of New Materials Engineering, Daejeon University, Korea in 2018. He is currently a Ph.M. candidate in the Nano & Information Materials Laboratory, Department of Chemical Engineering, Konkuk University, Republic of Korea under Prof. Doo Kyung Moon's supervision. His research interests are in organic materials, conjugated polymers and piezoelectric nanogenerators.

Hyoung Seok Lee received his B.S. degree from the Department of Materials and Chemistry Engineering, Konkuk University, Republic of Korea in 2018. He is currently a Master candidate in the Nano & Information Materials Laboratory (NIMs), Department of Chemical Engineering, Konkuk University, Korea under Prof. Doo Kyung Moon's supervision. His research focuses on the fabrication and characterization of organic hybrid electronic devices.

Doo Kyung Moon received his Ph.D. from Tokyo Institute of Technology, Japan in 1993, and had post-doc experience at the University Arizona in USA (1993–1994) and the Korea Institute of Science and Technology (KIST, 1994–1995). Now, he is a professor of the Department of Chemical Engineering, Konkuk University, Republic of Korea. He was an adjunct professor of Advanced Industrial Science and Technology (AIST, 2009–2010). His research group works on the development of organic materials and organic electronic devices for organic solar cells, organic light emitting diodes and piezoelectric nanogenerators. For details please see the lab website: http://nanoscience.or.kr.